Self-organization of Ge islands on high-index Si substrates

Hiroo Omi* and Toshio Ogino
NTT Basic Research Laboratories, Atsugi, Kanagawa, 243-0198, Japan
(Received 28 August 1998; revised manuscript received 7 December 1998)

Films of Ge were grown on Si(113) and Si(331) substrates by molecular-beam epitaxy (MBE). We found that the Ge films grow in the Stranski-Krastanow (SK) mode on both substrates. The SK islands are bounded by facet planes, and have a wirelike shape on Si(113) and a dotlike shape on Si(331). The resulting island shapes are stable equilibrium ones, and are strongly governed by the mechanism of anisotropic strain relief. Moreover, multilayers of coherent Ge islands were stacked on a Si(113) substrate with spacer layers of Si by MBE. In the multilayers of Ge/Si, the wirelike Ge islands become more uniform as the number of layers is increased at a growth temperature of 400 °C. When the temperature is 450 °C, the shape of the islands changes from wirelike in the first Ge layer to dashlike in the sixth Ge layer. This temperature-dependent self-organization is caused by inhomogeneous strain distributions induced by the buried Ge islands that are vertically aligned in the Ge/Si multilayers. [S0163-1829(99)09911-7]

I. INTRODUCTION

Low-dimensional nanostructures, such as quantum wires and quantum dots, have become critical in the semiconductor science and technology field because they have great potential in optoelectronic and microelectronic devices.[1] Consequently, various methods for creating them have been proposed. The most common one involves using lithographic techniques for one- or two-dimensional nanostructure patterning. However, these techniques have disadvantages such as low throughput and essentially involve complex serial processing.

Due to its process- and damage-free features, structural self-organization has received much attention as a way to overcome these problems.[2–8] Of particular importance is the formation of coherent three-dimensional islands during epitaxial growth in lattice-mismatched materials, including Ge/Si and In(Ga)As/GaAs, by molecular-beam epitaxy and metal-organic chemical-vapor epitaxy.[9,10] These islands have usually been grown on low-index substrate surfaces, and their growth has been extensively studied from experimental[11] and theoretical[12,13] viewpoints. More recently, the study of self-organization has been extended to the use of high-index surfaces, particularly in compound semiconductor systems, and there has been some success in obtaining various types of nanostructures that have unique electrical and optical properties.[14,15] However, regarding Ge/Si systems, most previous work has focused on the growth of Ge on Si(100) and Si(111) substrates, and little attention has been paid to Ge growth on high-index Si substrates.

It is well known that facets with high-index mirror planes form on low-index Si substrates. Of these facets, (113) and (331) are particularly interesting because of their thermal stability. The (113) facet is one of the most stable, and is usually observed during high-temperature annealing of patterned Si(111) and Si(100) substrates. On the other hand, the (331) facet is stable on a vicinal Si(111) surface misoriented toward the $[11\bar{2}]$ direction.[16] These facets are therefore good candidates for forming high-index surfaces on a low-index Si substrate. The interest in these high-index planes also stems from the possibility that the growth of Ge islands on them could be tied in with that on the conventional low-index Si substrates in wafer-scale nanointegrations.[17]

On the other hand, it has been pointed out that self-assembled coherent islands have two inherent problems. One is fluctuation in the size of the islands, and the other is their random distribution over the surface. For instance, large surface migration in the island growth leads to a very inhomogeneous distribution of island size and random arrangements. These problems have to be solved for device applications. Fortunately, a stress-induced self-organization phenomenon has been found to occur during molecular-beam epitaxy (MBE) of strained Si/SiGe/Si multilayers on vicinal Si(100) substrates.[18] By utilizing this phenomenon, regular and uniform nanoscale SiGe dots can be obtained, and the process of self-organization can be controlled by tuning layer thickness, alloy composition, and substrate miscut. A self-organization mechanism was proposed in Refs. 19–21 on the basis of an elasticity theory. The structural details of the self-organized Ge dots in the Si/Ge/Si(100) multilayers have been studied by high-resolution x-ray diffraction[22] and cross-sectional transmission-electron microscopy (XTEM).[23]

In this paper, we report on Ge-island growth on Si(113) and (331) substrates. We extend the stress-induced self-organization to the self-assembly of Ge islands grown on a Si(113) substrate in order to obtain arrays of Ge islands with uniform size and shape. We show that Stranski-Krastanow (SK) growth of Ge films on both substrates produces self-assembled coherent Ge islands, and the Ge islands have a wirelike shape on Si(113) and a dotlike shape on Si(331). Moreover, we demonstrate that at appropriate substrate temperatures the stress-induced self-organization in Si/Ge/Si(113) multilayers produce wire-shaped Ge islands with a uniform size and dashlike Ge islands.

II. EXPERIMENT

Experiments were carried out in an MBE growth chamber equipped for reflection high-energy electron diffraction

(RHEED). Si and Ge were deposited by a 10-kV electron-beam evaporator and a boron-nitride Knudsen cell, respectively. Substrates were heated by a W filament placed behind the sample. Substrate temperature was measured by a pyrometer within an uncertainty of 30 °C. The thicknesses of the Si and Ge thin films were measured with quartz-crystal monitors calibrated by using RHEED oscillations during homoepitaxial growth on Si(111). The ultimate pressure of the chamber was 3×10^{-11} Torr, and the respective pressures when evaporating Si and Ge were below 3×10^{-9} and 5×10^{-10} Torr.

The substrates were Si(113) and Si(331) wafers (P doped, $\rho=1-10\,\Omega$ cm) cut into 14×16-mm^2 sections. The Si(113) substrate was miscut by 0.5°–1° almost along the $[33\bar{2}]$ direction, and the Si(331) substrate had unintentional misorientation of about 0.2° almost along the $[11\bar{6}]$ direction. The substrates were initially cleaned by repeated oxidation in H_2SO_4:H_2O_2=1:4 solutions and oxide removal in HF solution, and protective oxides were formed using HCl:H_2O_2:H_2O=1:1:5 solutions at the final stage. After outgassing at 620 °C for 1–2 h, the samples were heated to 860 °C to remove the protective oxides. The samples were then cooled to the Si buffer-growth temperature of 620 °C. Si buffer layers were deposited at 1.0 nm/min. After growing 20–200 nm of Si buffer layers, the samples were heated to the growth temperatures of single Ge layers or Ge/Si multilayers.

Single layers of Ge were grown on Si(113) and (331) substrates in the substrate temperature range of 200–700 °C. Their thicknesses were varied within 10 nm. The film thicknesses are given in ML; 1 ML corresponds to a 0.164-nm thickness on Si(113) or a 0.125-nm thickness on Si(331). Ge deposition rates were 0.7 ML/min on Si(113) and 1.2 ML/min on Si(331). Ge/Si multilayers were grown only on Si(113) substrates at 400 and 450 °C. Respective deposition rates were 0.6 ML/min for Ge and 5 ML/min for Si. The thickness of individual Ge layers was maintained at 6.4 ML, and that of the Si layers was varied from 30 to 60 ML. The multilayers contain up to 20 periods.

Surface morphology was observed by tapping-mode atomic force microscopy (AFM) in air. RHEED specular beam intensities were measured by a photodiode device placed in front of a fluorescent screen. XTEM images were obtained at an incident-beam energy of 300 kV.

III. RESULTS

A. Growth of Ge on high-index Si substrates

1. Ge on Si(113)

Figure 1 shows a representative profile of RHEED specular beam intensity obtained during the growth of Ge on Si(113) at a substrate temperature of 400 °C. The intensity oscillates with a period corresponding to nearly 1-ML thickness, but its amplitude decreases with increasing Ge film thickness. The oscillation continues until the corresponding monolayer thickness of 5 ML, and then the intensity of oscillation is damped. This profile is indicative of the transition from layer-by-layer growth to three-dimensional island growth (i.e., the SK mode) at this temperature.

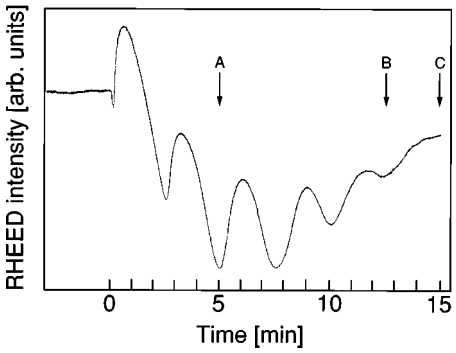

FIG. 1. RHEED intensity oscillation during the growth of Ge on Si(113) substrates at 400 °C. The growth rate of Ge was estimated to be 0.34 ML/min from the oscillations. The incident electron beam was parallel to the $[33\bar{2}]$ direction. *A*, *B*, and *C* correspond to AFM images (a), (b), and (c) in Fig. 2.

To obtain more information about the growth mode transition, we observed AFM images as a function of Ge film thickness. Figure 2 shows the AFM images obtained at Ge film thicknesses of 2, 5, 6.4, and 11 ML (*A*, *B*, *C*, and *E* in Fig. 1). In Fig. 2(a), the bright and dark areas correspond to higher and lower terraces, respectively. The height difference between these areas is about 0.2 nm, which is nearly equal to

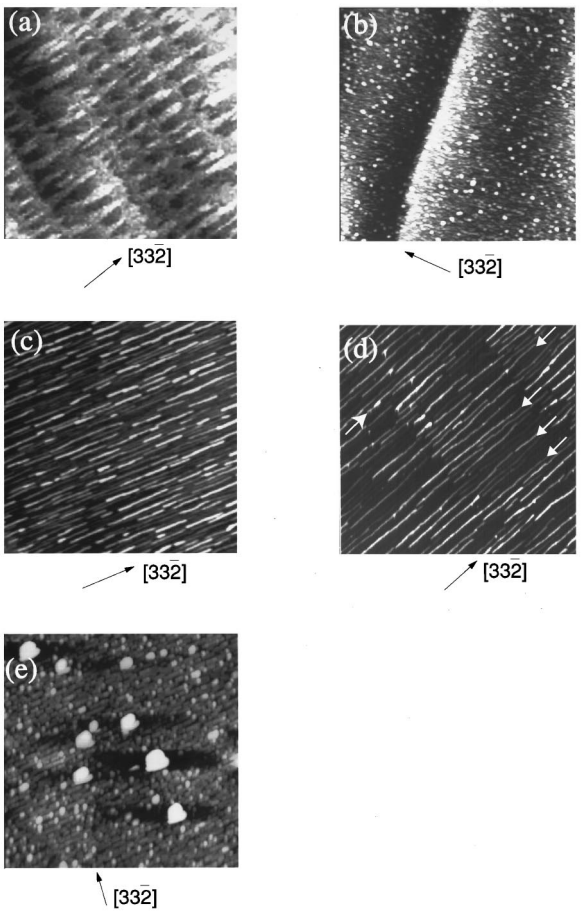

FIG. 2. AFM image evolution of Ge films grown on Si(113) at 400 °C: (a) 2 ML, (b) 5 ML, (c), (d) 6.4 ML, and (e) 11 ML. The scan area is 1×1 μm^2 in (a), (b), (c), and (e), and 2×2 μm^2 in (d). The height range is 5 nm.

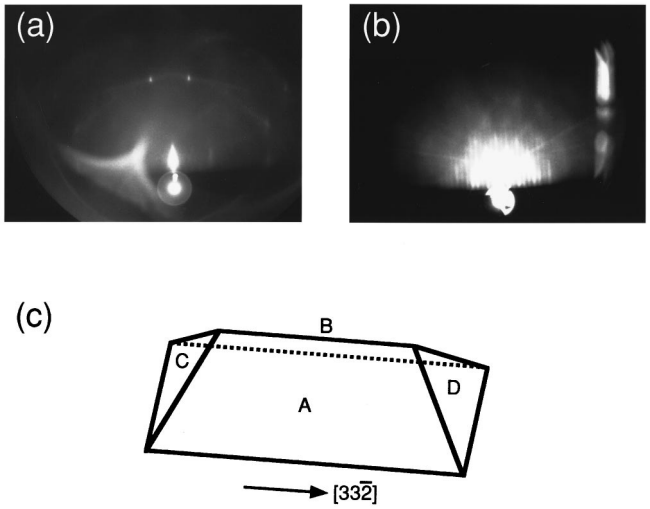

FIG. 3. (a) RHEED patterns of the sample in Fig. 2(b) taken along (a) $[33\bar{2}]$ and (b) $[1\bar{1}0]$. (c) Model of a wire-shaped Ge island.

the single step height (0.164 nm) of the substrate. Therefore, this AFM image confirms the presence of Ge wetting layers on the substrate. Notice that the topmost terraces are elongated in the $[33\bar{2}]$ direction perpendicular to the step edges on the lower terraces, and most of them make contact with the step edges. This anisotropy is possibly responsible for the formation of surface reconstruction of the Ge overlayers, in which elastic strains are more easily relieved along the $[1\bar{1}0]$ direction than in the $[33\bar{2}]$ direction, as mentioned in Ref. 24. When the Ge film exceeds a critical thickness of 5 ML, as seen in Fig. 2(b), Ge islands having a relatively round shape start to grow randomly on the terrace of the wetting layers. Further depositions, however, result in a drastic transition of island shape. In Fig. 2(c), the nanoscale Ge islands elongate along the $[33\bar{2}]$ direction and cover the entire surface contiguously. Careful AFM observations reveal that the island arrangement does not originate from steps on the surface because most steps are normal to the direction of the elongation. Interestingly, most islands near the steps appear as if they grew continuously across the steps, as indicated by the arrows in Fig. 2(d). Some are extraordinarily long, having submicron length. This finding clearly indicates a positional correlation between the islands on the upper terrace and the islands on the lower terrace at the steps. The correlation probably originates in the Ge-island-induced strain fields in the substrate through the steps. This is, to our knowledge, the first observation of island self-ordering beyond the steps. Upon further depositions of Ge films, large islands (about 200 nm in diameter and about 50 nm in height) formed on the surface [Fig. 2(e)].

Now we turn to the details of the self-assembled wire-shaped Ge island features. Figures 3(a) and 3(b) show the RHEED patterns obtained from the surface shown in Fig. 2(c). The RHEED pattern for the $[33\bar{2}]$ direction is shaped like an arrowhead [Fig. 3(a)], while that for the $[1\bar{1}0]$ direction has normal reflection spots on blurry streaks [Fig. 3(b)]. This indicates that the elongated ridges of the islands are bounded by facets. A model of the island is schematically shown in Fig. 3(c). The arrowhead angle of 14° with respect

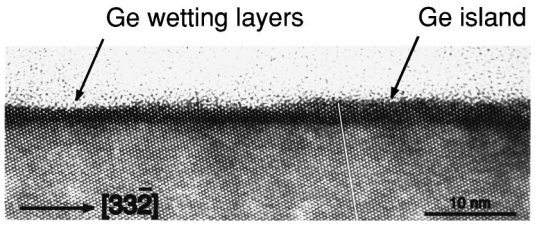

FIG. 4. Cross-sectional TEM image of the sample in Fig. 1 viewed in the $[1\bar{1}0]$ projection. The white line is simply a guideline.

to the surface normal direction indicates that facets *A* and *B* in Fig. 3(c) are oriented in the {159} direction.

Figure 4 is a cross-sectional TEM image of the sample in Fig. 2(c). The lattice image taken along the $[1\bar{1}0]$ zone axis shows that no dislocations exist at the Ge/Si interface or inside the Ge wetting layers and islands. This clearly indicates that the wire-shaped Ge islands are coherent to the Si substrate.

Next we explored the growth conditions under which the wire-shaped islands formed on the surface. Figure 5 shows the dependence of the Ge growth mode on the substrate temperature and Ge film thickness. As is evident from this figure, when we used 5–8-ML coverage the wire-shaped islands were obtained between 400 and 500 °C. Also apparent is that the formation of the islands depends on both Ge coverage and growth temperature. This dependence indicates that a kinetic process is involved in their formation.

We characterized the size distribution of the Ge nanowires as a function of Ge coverage and growth temperature. The island width and length distributions, as obtained from the AFM images, are shown in Fig. 6(a) for Ge thicknesses

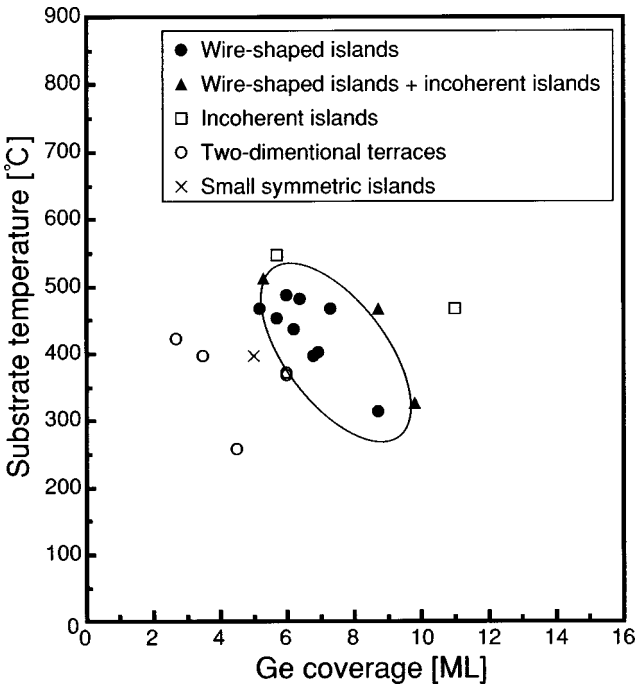

FIG. 5. Morphology of Ge films grown on the Si(113) substrate as a function of Ge coverage and substrate temperature. The enclosed area represents the region in which wire-shaped Ge islands are formed.

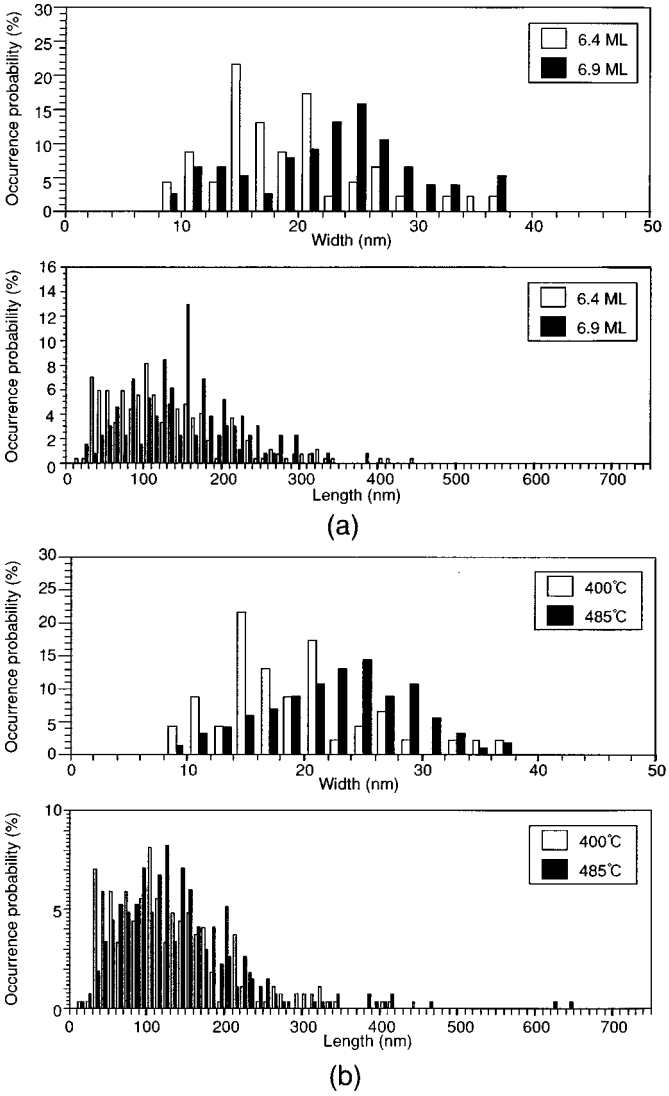

FIG. 6. Typical distributions of the base width along $[1\bar{1}0]$ and length along $[33\bar{2}]$ of the Ge wire-shaped islands grown on Si(113) substrates: (a) 6.4- and 6.9-ML Ge coverages, and (b) 400 and 485 °C substrate temperatures. Note that these dimensions were determined by AFM measurements. The Ge growth rate was fixed at 0.7 ML/min. The size distributions have peaks (marked by arrows).

of 6.4 and 6.9 ML at the fixed substrate temperature of 400 °C. The average island length and width increase from 20 to 24 nm and from 137 to 159 nm, respectively, with increasing Ge coverage from 6.4 to 6.9 ML at 400 °C. The coverage-dependent changes in the size of the islands were also observed within the range of 5–8 ML. Shown in Fig. 6(b) are distributions of island sizes for growth temperatures of 400 and 485 °C with a fixed Ge coverage of 6.4 ML. Increasing the substrate temperature from 400 to 480 °C also resulted in the increase in width and length from 20 to 24 nm and from 137 to 148 nm, respectively, at a fixed Ge coverage of 6.4 ML. However, when the growth temperature is above 500 °C, large incoherent islands grow on the surface (Fig. 5). The above results suggest that the sizes of the wire-shaped islands can be changed by adjusting Ge coverage and growth temperature. The width and length distributions, however, are quite large. The reducing fluctuation of the island size is described in a later section.

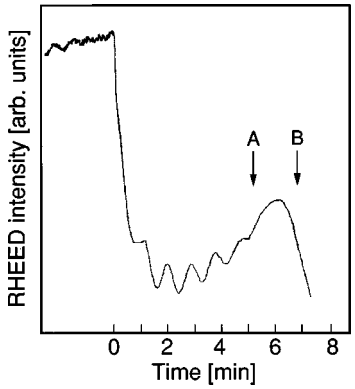

FIG. 7. The RHEED intensity oscillations during the growth of Ge on a Si(331) substrate at 400 °C. The growth rate of Ge was 1.2 ML/min. The incident electron beam was parallel to the $[11\bar{6}]$ direction. The letters *A* and *B* correspond to the AFM images in Figs. 8(a) and 8(b).

2. Ge on Si(331)

Figure 7 shows the RHEED intensity profile during the growth of Ge on Si(331) at a substrate temperature of 400 °C. The intensity oscillations continue up to about 4 ML and then the intensity of oscillations is damped. This clearly indicates that, like Ge growth on Si(113), Ge growth on Si(331) proceeds in the SK growth mode. Figures 8(a) and 8(b) show AFM images of the Ge islands obtained at Ge film thicknesses of 6 and 8.4 ML (*A* and *B* in Fig. 7). Bright regions indicate Ge islands. As clearly seen in Fig. 8(a), the Ge islands have a round shape and are distributed over the surfaces. Typical Ge-island width and height distributions are in the range of 15–40 and 0.6–2.8 nm, and the averages are 23.7 nm (width) and 1.6 nm (height), and the island spacing is eventually 20–30 nm. The island density is $2.0 \times 10^{11}\,\mathrm{cm}^{-2}$. The islands remain round and their size and density increase with Ge coverages ranging from 5 to 8 ML at 400 °C. A magnified view of a typical island and the model derived from the image are shown in Figs. 8(c) and 8(d), respectively. In the model, the Ge island is bounded by several facet planes forming a peak. RHEED patterns obtained from the surface shown in Fig. 9(a) reveal that the Ge islands have {221} and {11,13,4} facet planes. The RHEED patterns also indicate that the islands are symmetric with respect to the $[11\bar{6}]$ direction and asymmetric with respect to the $[1\bar{1}0]$ direction. It should be noted, however, that some islands are aligned along steps on upper terraces, as indicated by the arrow in Fig. 8(a). This alignment is probably due to the presence of energy barriers at steps for blocking the surface diffusion of Ge atoms. When a diffusion barrier exists at the higher side of the steps, the density of the Ge atoms there is larger than that at the lower side of the steps. Thus, the nucleation probability is increased at the upper sides of the steps. Beyond 8 ML, we observed large, high islands in addition to the round islands [Fig. 8(b)]. RHEED and AFM studies on Ge growth on Si(331) substrates observed coherent SK growth at substrate temperatures ranging from 400 to 450 °C at coverages of 5–9 ML.

Figure 10(a) shows an XTEM image of the sample in Fig. 8(b). The most important feature in this image is that the round islands (*A* in Fig. 10) have no dislocations, while the

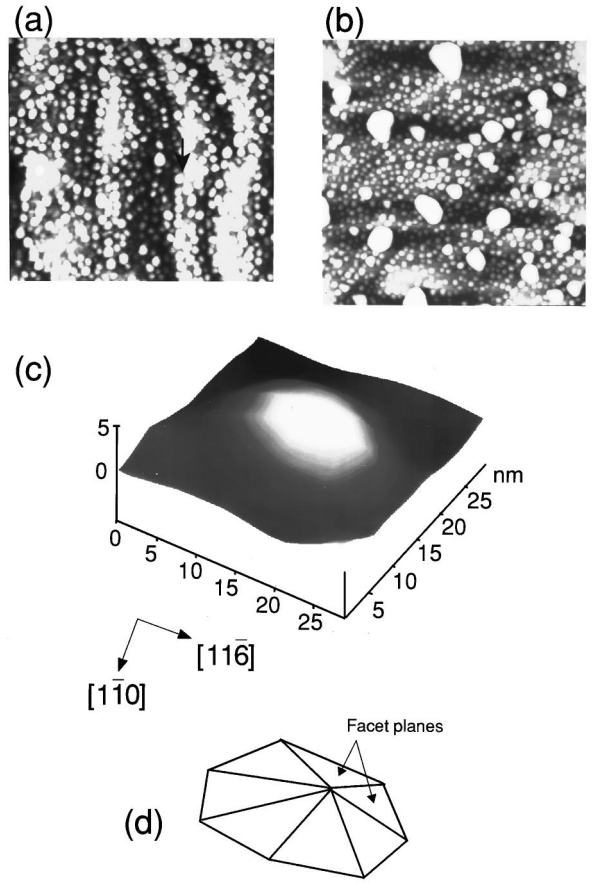

FIG. 8. AFM images of Ge islands grown at (a) 6- and (b) 8.4-ML coverages on Si(331) substrates at 400 °C. Scan areas are $600\times600\,\mathrm{nm}^2$ in (a), and $1\times1\,\mu\mathrm{m}^2$ in (b). The height range is 5 nm. (c) Magnified AFM image of a coherent Ge island on Si(331). (d) Model of the coherent Ge island on a Si(331) substrate.

large island (*B* in Fig. 10) has a dislocation at the Ge/Si interface. The dislocation is indicated by an arrow in the magnified view of the outlined area [Fig. 10(b)]. In addition, the TEM image showed that the dislocated island has {111} facet planes inclined by 22° with respect to the (331) surface.

3. Stability of the coherent Ge islands on Si(113) and (331) surfaces

It has been reported that the stability of the islands that can grow depends sensitively on the stress and coverage.[25–27]

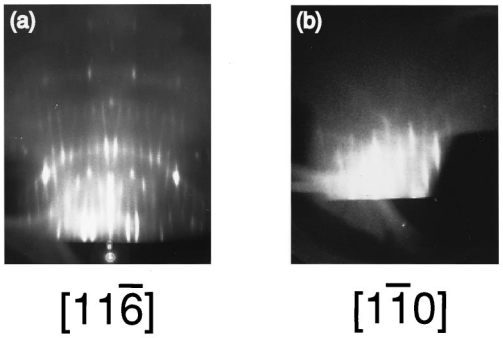

FIG. 9. (a) RHEED patterns of the sample in Fig. 8(a) taken along (a) [11$\bar{6}$] and (b) [1$\bar{1}$0].

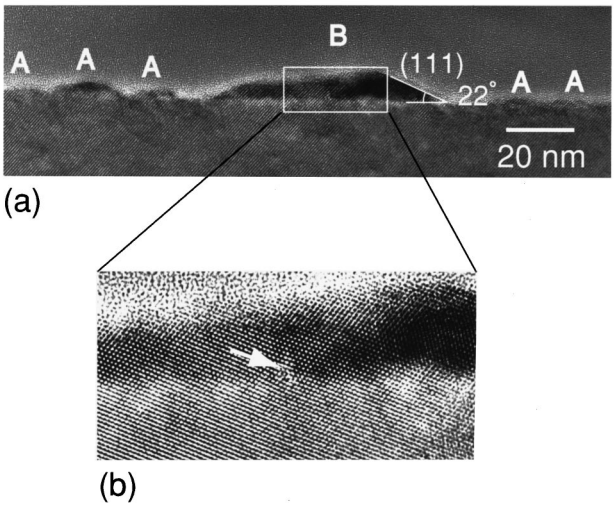

FIG. 10. (a) Cross-sectional TEM image of the sample in Fig. 8(b) viewed along the [1$\bar{1}$0] direction. (b) Magnification of the outlined area in (a). The position of the dislocation is indicated by the white arrow. Islands labeled *A* and *B* are coherent and incoherent, respectively.

Daruka and Barabási[27] recently presented equilibrium phase diagrams for island formation that show lattice misfit and coverage on the basis of thermodynamical theory. In the phase diagram, they showed that SK growth can provide two different types of islands on the wetting layers. One is a stable island and the other is an unstable ripening island. Therefore, it is important to address the stability of the coherent islands on the (113) and (331) surfaces. To reveal the stability of the islands, we performed a series of annealing experiments for coherent islands that were grown on the both surfaces at 400 °C as a function of annealing time. The results show that the annealings at the temperatures of 400, 450, and 500 °C for 1 h and 30 min did not significantly change the island shapes and their distributions. We also could not find any evidence of island coalescence on the surfaces. These results indicate that the coherent islands that we obtained are stable equilibrium shapes—not ripening or metastable ones.

B. Self-organization of Ge islands in Si/Ge/Si(113) multilayers

Figure 11 shows AFM images of (a) a single layer of Ge and (b) the 11th Ge layer of a Ge/Si multilayer structure grown on a Si(113) substrate at 400 °C. Bright regions indi-

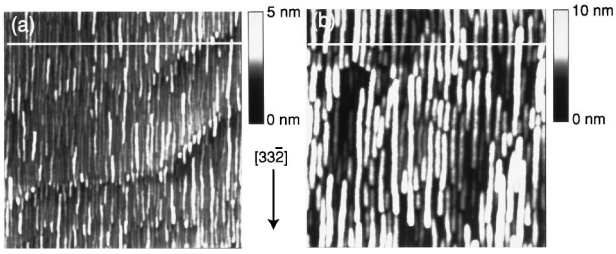

FIG. 11. AFM images of Ge islands grown at 400 °C: (a) grown on Si(113) substrates; (b) grown on 11 layers of Ge islands/Si multilayers. The image size is $1\times1\,\mu\mathrm{m}^2$. Note that the Ge islands become large and uniform with the formation of multilayers.

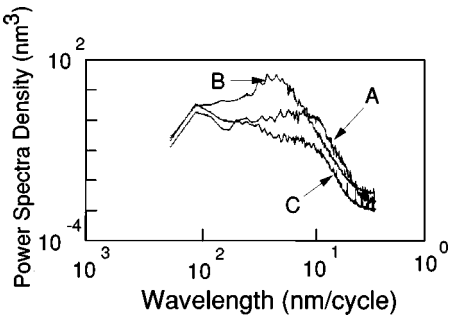

FIG. 12. Power density spectra obtained along the $[1\bar{1}0]$ direction from the Ge surface of (*A*) Ge(6.4 ML)/Si, (*B*) Ge(6.4 ML)/{Si(30 ML)-Ge(6.4 ML)}×10/Si, and (*C*) Ge(6.4 ML)/{Si(60 ML)-Ge(6.4 ML)}×10/Si.

cate Ge islands. Nanoscale wire-shaped islands along the $[33\bar{2}]$ direction cover both entire surfaces [Figs. 11(a) and 11(b)]. For the single Ge layer [Figs. 11(a) and 2(c)], as mentioned in Sec. III A 1, the islands have a prismlike shape with {159} facets, and their average width, length, and height are 20, 137, and 0.7 nm, respectively, at the 6.4-ML Ge thickness. As the number of Ge/Si bilayers was increased, the island size became more uniform, as can be seen in Fig. 11(b), with the wirelike shape retained. RHEED patterns obtained from individual Ge layers indicate that the {159} facets were maintained throughout. On average, the islands of the 11th Ge layer were 30 nm wide, 150 nm long, and 3 nm high. This clearly indicates that the islands become larger because of the multilayer stacks. The nanowire density was decreased from approximately 60 lines/μm for the first Ge layer to about 30 lines/μm for the 11th Ge layer.

We confirmed the size uniformity of Ge islands by measuring power density spectra (PDS) from the resulting surfaces. In general, PDS give us information about the periodicity of island arrangement. Figure 12 shows PDS obtained from the surface along the $[1\bar{1}0]$ direction. The $[1\bar{1}0]$ direction is perpendicular to the direction of island elongation, as indicated by the white lines in Figs. 11(a) and 11(b). Spectrum *A* is from the first Ge layer and *B* is from the 11th Ge layer. As clearly see, spectrum *A* (with a broad peak at 20 nm) changes to spectrum *B* (with a sharp peak at 30 nm) as a consequence of multilayer stackings. This indicates that the Ge islands are remarkably ordered into a 30-nm periodicity, implying that stress-induced self-organization occurred in this system. This result is in good agreement with the theoretical prediction that the Si spacer layer acts as a bandpass filter in this self-organization.[17] For further confirmation of about the self-organization, we measured the spectrum from the 11th Ge layer at the Si layer thickness of 60 ML. Spectrum *C* is from the 11th Ge layer surface, with an individual Si layer thickness of 60 ML. Comparing spectra *B* and *C* in Fig. 12, we see that the increased Si thickness certainly leads to a broad distribution in periodicity, indicating a much less pronounced self-organization. Consequently, we can say that Ge nanowires with uniform width were obtained by the stress-induced self-organization phenomenon at 400 °C. This claim is further supported by the XTEM observations, which are discussed below.

Figure 13 shows AFM images of (a) a single layer of Ge film and (b) the sixth Ge layer of a Ge/Si multilayer structure

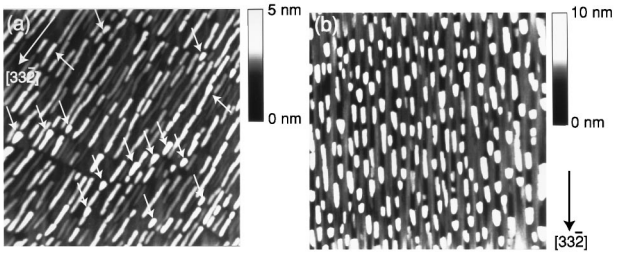

FIG. 13. AFM images of Ge islands grown at 450 °C: (a) on Si substrates, (b) on six layers of Ge islands/Si multilayers. The image size is 1×1 μm^2. Short, high Ge islands are indicated by arrows.

grown at 450 °C. For the first Ge layer, increasing the substrate temperature by 50 °C results in the emergence of relatively short Ge islands with increased width and height, as indicated by the arrows in Fig. 13(a). But as the number of Ge/Si bilayers increases, the island size and shape drastically change: the resulting Ge islands on the first Ge layer are long and wirelike [Fig. 13(a)], but short and wirelike or dashlike on the sixth Ge layer [Fig. 13(b)]. The length-to-width ratio of the Ge islands approximately decreased from 6 for the first Ge layer to 2 for the sixth Ge layer. On average, the sixth Ge layer islands were about 35 nm wide, 82 nm long, and 3 nm high.

The above AFM results clearly indicate that the self-organization of Ge nanowires depends on the growth temperature. To reveal the origin of this temperature dependence, we examined multilayer samples by XTEM. Figures 14(a) and 14(b) show XTEM images of a sample grown at 400 °C and Figs. 14(c) and 14(d) show images of one grown at 450 °C. These images were taken along the island elongation direction of $[33\bar{2}]$ and the perpendicular direction of $[1\bar{1}0]$. Dark and bright regions are Ge and Si layers, respectively. As is apparent in these images, Ge islands are vertically aligned with no dislocation defects, such as ''conical shaped defects,'' in the Si/Ge/Si(100) multilayers[28] at both temperatures. However, the detailed alignment features are different at 400 and 450 °C. At 400 °C, the Ge island gradually increases in size with increasing Ge/Si bilayer number, while keeping its long wirelike shape [Fig. 14(b)]. Moreover, new island stackings emerged during the multilayer stacking, as indicated by the arrows in Fig. 14(b). At 450 °C, on the other hand, relatively short Ge islands appear in the first layer and their height and width progressively increase as the number of Ge island stacks increases [Figs. 14(c) and 14(d)].

IV. DISCUSSIONS

A. Shape of the SK Ge islands on high-index Si substrates

For Ge islands on Si(113), as mentioned in Sec. III A 1, we observed an anisotropic elongation in the $[33\bar{2}]$ direction. The anisotropy can be explained as follows. Tersoff and Tromp[29] calculated the energy of a coherently strained island considering its growth kinetics, and found that the strained island experiences a shape transition from dotlike to wirelike in order to compensate for elastic strain as it grows beyond a critical size. We actually observed such shape transition in Ge islands at coverages between 5 and 6.4 ML at 400 °C [compare Figs. 2(b), 2(c), and 2(d)]. Consequently, the

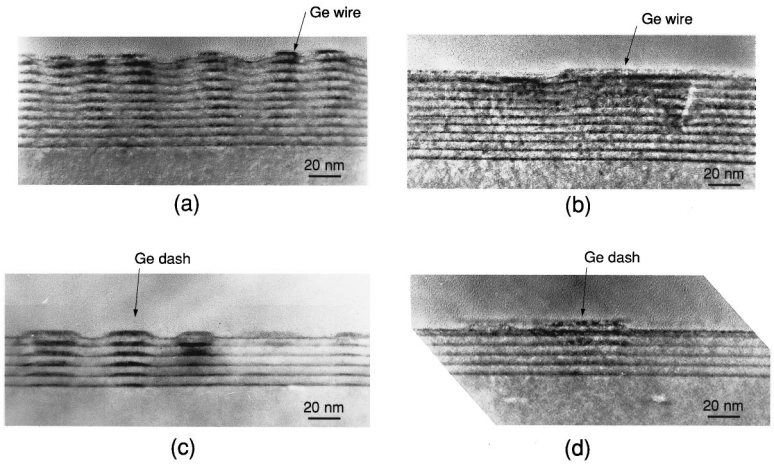

FIG. 14. (a) and (b) Cross-sectional TEM images of the Ge(6.4 ML)/{Si(30 ML)-Ge(6.4 ML)}×9/Si multilayer grown at 400 °C. (c) and (d) Ge(6.4 ML)/{Si(60 ML)-Ge(6.4 ML)}×9/Si multilayer grown at 450 °C. The images are viewed along the $[1\bar{1}0]$ [(a) and (c)] and $[33\bar{2}]$ [(b) and (d)] directions. The samples were capped with amorphous Si after stacking the Ge/Si multilayers.

anisotropic shape can be explained by the strain-relief mechanism proposed by Tersoff and Tromp. In the discussion of island shape, we should address the orientation of elongated islands. Recently, Caro and Tapfer[30] calculated, on the basis of classical elasticity theory, the lattice deformation of semiconductor epitaxial layers grown commensurately on an arbitrarily oriented surface without defects and dislocations. They found that tetragonal and shear strains occur in coherent films on low-symmetry cubic substrate surface, and that the value of the shear strain is highest along the $[33\bar{2}]$ direction on a (113) surface. These findings are not dependent on epitaxial layer-substrate material combinations. Elasticity theory predicts noticeable lattice deformation in Ge wetting layers in the $[33\bar{2}]$ direction, implying that compressive strain in Ge film caused by the Si(113) substrate can relax in the $[33\bar{2}]$ direction. A similar situation is expected in Ge islands. In fact, we have confirmed anisotropic relaxation in islands by elastic simulations based on empirical potentials.[31] (Details of the simulations will be described elsewhere.) Consequently, it is energetically favorable for strained Ge islands beyond a critical size to elongate in the $[33\bar{2}]$ direction. In addition, Tersoff and Tromp also mentioned, in Ref. 29, that if the island is anisotropically strained it should be normally oriented with respect to the direction of maximum strain. Accordingly, the stresses imposed by the substrate along the $[1\bar{1}0]$ direction can be considered to be larger than those along the $[33\bar{2}]$ direction in the Ge island. Careful examination of the lattice image in Fig. 5 reveals that the Ge island lattices seem to gradually distort along the $[33\bar{2}]$ direction as the island height increases, as indicated by the white line parallel to a crystallographic axis. This further suggests that the Ge islands are anisotropically strained. Moreover, confirming the lattice deformation will require a more detailed study.

On Si(331), on the other hand, coherent Ge islands have a relatively round shape. This finding supports our discussion of anisotropic shape of Ge islands on Si(113). According to the elastic theory in Ref. 30, the shear strain value in Ge wetting layers on the (331) surface is lower than that on the (113) surfaces. This implies that, unlike Ge islands on Si(113), the Ge islands on Si(331) have no particular orientation in which their stress can be easily relieved. This is likely to lead to the formation of Ge islands with a relatively round shape.

B. Mechanism of self-organization in Si/Ge/Si(113) multilayers

Finally, we discuss the origin of the temperature-dependent self-organization of Ge islands on {Si/Ge}/Si(113) multilayers. Figure 15 schematically shows how the self-organizations occurred at the two different substrate temperatures. The shape difference in the self-organized Ge islands can be explained as follows. For the first Ge layer grown at 450 °C, there are many short, wide, and high wire-like islands together with long wire-shaped islands [Fig. 13(a)]. The short wirelike islands were not observed in the first Ge layer grown at 400 °C [Fig. 11(a)]. When the Si spacer layer caps the first Ge layers with the short, high Ge islands, the strain field induced by the short islands on the capping Si layer surface is considered to be locally larger than that induced by the long wires, as illustrated by dashed lines in Fig. 15. Since most of the atoms are driven toward

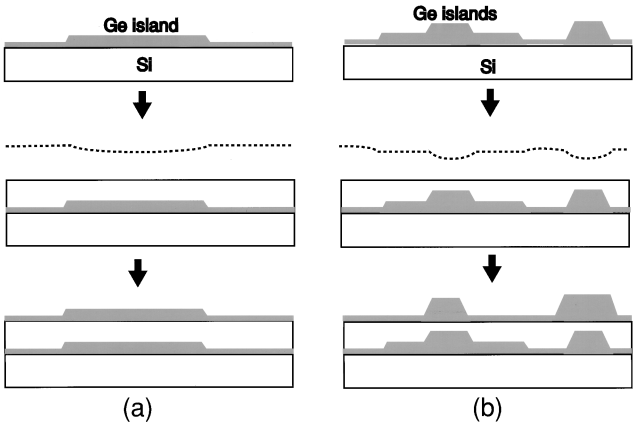

FIG. 15. Schematic illustration of the self-organization of Ge islands at (a) 400 °C and (b) 450 °C in Si/Ge/Si(113) multilayers. Dashed lines indicate the degree of surface potential induced by the first layer of Ge islands. Ge islands were vertically aligned.

the more energetically favorable region, the subsequent Ge islands preferentially grow in the more strained regions. Actually, the XTEM image taken along $[33\bar{2}]$ captured the vertical stacking of short Ge islands [Fig. 14(d)]. On the other hand, the first Ge layer grown at 400 °C does not contain the short, high islands observed at 450 °C [Fig. 14(b)]. Therefore, long islands produce a linearly uniform strain field on the subsequent Si space layer, resulting in the formation of uniformly sized nanowires [Fig. 15(a)].

V. SUMMARY

We have used molecular-beam epitaxy to extend the use of high-index Si substrates to self-assembly and self-organization of Ge islands. The SK growth mode produces stable and defect-free self-assembled Ge nanowires on a Si(113) substrate, and Ge nanodots on a Si(331) substrate. The different shape of the islands is related to the degree of anisotropic elastic relaxation of the strain that originates from the cubic anisotropy of the Si substrates. By stacking the Ge islands in Si/Ge/Si(113) multilayers, we are able to obtain Ge nanowires with uniform sizes at 400 °C. We also demonstrated that the shape of the self-organized Ge island changes from long-wire-like to short-wire-like or dashlike at 450 °C.

ACKNOWLEDGMENTS

We would like to thank Hiroki Hibino, Dr. Yasuo Kunii, Suguru Hoshino, Dr. Koji Sumitomo, Dr. Kuniyil Prabhakaran, Dr. Yoshihiro Kobayashi, Dr. Tsuneo Fukuda, and Dr. Yukihiro Hirota for their encouragement throughout this work, and we also thank Dr. Masataka Yamawaki for the TEM observations.

*Author to whom correspondence should be addressed. Electronic address: homi@will.brl.ntt.co.jp

[1] C. Weisbuch and B. Vinter, *Quantum Semiconductor Structures* (Academic, San Diego, 1991).
[2] H. Hibino, N. Shimizu, Y. Shinoda, and T. Ogino, in *Mechanisms of Thin Film Evolution*, edited by S. M. Yalisove, C. V. Thompson, and O. J. Eaglesham, MRS Symposia Proceedings No. 317 (Materials Research Society, Pittsburgh, 1994), p. 41.
[3] H. Hibino, N. Shimizu, and Y. Shinoda, J. Vac. Sci. Technol. A **11**, 2458 (1993).
[4] T. Ogino, H. Hibino, and K. Prabhakaran, J. Vac. Sci. Technol. B **14**, 4134 (1996).
[5] T. Ogino, H. Hibino, and Y. Homma, Appl. Surf. Sci. **107**, 1 (1996).
[6] M. Kitamura, M. Nishioka, J. Oshinowo, and Y. Arakawa, Appl. Phys. Lett. **66**, 3663 (1995).
[7] T. Arakawa, H. Watabe, Y. Nagamune, and Y. Arakawa, Appl. Phys. Lett. **69**, 1294 (1996).
[8] H. Sunamura, N. Usami, Y. Shiraki, and S. Fukatsu, Appl. Phys. Lett. **68**, 1847 (1996).
[9] R. Nötzel, Semicond. Sci. Technol. **11**, 1365 (1996).
[10] N. N. Ledentsov, V. A. Schukin, M. Grundmann, N. Kristaedter, J. Böhrer, O. Schmidt, D. Bimberg, V. M. Ustinov, A. Y. Egorov, A. E. Zhukov, P. S. Kop'ev, S. V. Zaitsev, N. Y. Gordeev, Z. I. Alferov, A. I. Borovkov, A. O. Kosogov, S. S. Ruvimov, P. Werner, U. Gösele, and J. Heydenreich, Phys. Rev. B **54**, 8743 (1996).
[11] Y.-W. Mo, D. E. Savage, B. S. Swarzentruber, and M. G. Lagally, Phys. Rev. Lett. **65**, 1020 (1990).
[12] Y. Chen and J. Washburn, Phys. Rev. Lett. **77**, 4046 (1996); Phys. Rev. Lett. **78**, 3028 (1997).
[13] I. Daruka and A.-L. Barabási, Phys. Rev. Lett. **78**, 3027 (1997).
[14] R. Nötzel, N. N. Ledentsov, L. Daweeritz, and K. Ploog, Phys. Rev. B **45**, 3507 (1992).
[15] R. Nötzel, J. Temmyo, and T. Tamamura, Nature (London) **369**, 131 (1994).
[16] H. Hibino, T. Fukuda, M. Suzuki, Y. Homma, T. Sato, M. Iwatsuki, K. Miki, H. Tokumoto, Phys. Rev. B **47**, 13 027 (1993); H. Hibino and T. Ogino, *ibid.* **53**, 15 682 (1996).
[17] T. Ogino, Surf. Sci. **386**, 137 (1997).
[18] C. Teichert, M. G. Lagally, L. J. Peticolas, J. C. Bean, and J. Tersoff, Phys. Rev. B **53**, 16 334 (1996); F. Liu and M. G. Lagally, Surf. Sci. **386**, 169 (1997).
[19] J. Tersoff, C. Teichert, and M. G. Lagally, Phys. Rev. Lett. **76**, 1675 (1996).
[20] S. Christiansen, M. Albrecht, and H. P. Strunk, Comput. Mater. Sci. **7**, 213 (1996).
[21] V. A. Shchukin, D. Bimberg, V. G. Malyshkin, and N. N. Ledentsov, Phys. Rev. B **57**, 12 262 (1998).
[22] A. A. Dahuber, P. Schittenhelm, V. Holy, J. Stangl, G. Bauer, and G. Abstreiter, Phys. Rev. B **55**, 15 652 (1997).
[23] E. Mateeva, P. Sutter, J. C. Bean, and M. G. Lagally, Appl. Phys. Lett. **71**, 3233 (1997).
[24] J. Knall and J. B. Pethica, Surf. Sci. **265**, 156 (1992).
[25] G. Medeiros-Ribeiro, A. M. Bratkovski, T. I. Kamis, D. A. A. Ohlberg, and R. S. Williams, Science **279**, 353 (1998); G. Medeiros-Ribeiro, T. I. Kamis, D. A. A. Ohlberg, and R. S. Williams, Phys. Rev. B **58**, 3533 (1998).
[26] J. A. Floro, G. A. Lucadamo, E. Chason, L. B. Freund, M. B. Sinclair, R. D. Twesten, and R. Q. Hwang, Phys. Rev. Lett. **80**, 4717 (1998); J. A. Floro, E. Chason, M. B. Sinclair, L. B. Freund, and G. A. Lucadamo, Appl. Phys. Lett. **73**, 951 (1998).
[27] I. Daruka and A.-L. Barabási, Phys. Rev. Lett. **79**, 3708 (1997); I. Daruka and A.-L. Barabási, Appl. Phys. Lett. **72**, 2102 (1998).
[28] E. Carlino, C. Giannini, C. Gerardi, L. Taper, K. A. Mader, and H. von Kanel, J. Appl. Phys. **79**, 1441 (1996).
[29] J. Tersoff and R. M. Tromp, Phys. Rev. Lett. **70**, 2782 (1993).
[30] L. D. Caro and L. Tapfer, Phys. Rev. B **48**, 2298 (1993).
[31] Y. Kunii, S. Hoshino, H. Omi, and T. Ogino (unpublished).